

Directional analysis of coherent oscillatory field potentials in the cerebral cortex and basal ganglia of the rat

Andrew Sharott¹, Peter J. Magill², J. Paul Bolam² and Peter Brown¹

¹Sobell Department of Motor Neuroscience and Movement Disorders, Institute of Neurology, Queen Square, London WC1N 3BG, UK

²Medical Research Council Anatomical Neuropharmacology Unit, University of Oxford, Mansfield Road, Oxford OX1 3TH, UK

Population activity in cortico-basal ganglia circuits is synchronized at different frequencies according to brain state. However, the structures that are likely to drive the synchronization of activity in these circuits remain unclear. Furthermore, it is not known whether the direction of transmission of activity is fixed or dependent on brain state. We have used the directed transfer function (DTF) to investigate the direction in which coherent activity is effectively driven in cortico-basal ganglia circuits. Local field potentials (LFPs) were simultaneously recorded in the subthalamic nucleus (STN), globus pallidus (GP) and substantia nigra pars reticulata (SNr), together with the ipsilateral frontal electrocorticogram (ECoG) of anaesthetized rats. Directional analysis was performed on recordings made during robust cortical slow-wave activity (SWA) and 'global activation'. During SWA, there was coherence at ~ 1 Hz between ECoG and basal ganglia LFPs, with much of the coherent activity directed from cortex to basal ganglia. There were similar coherent activities at ~ 1 Hz within the basal ganglia, with more activity directed from SNr to GP and STN, and from STN to GP rather than vice versa. During global activation, peaks in coherent activity were seen at higher frequencies (15–60 Hz), with most coherence also directed from cortex to basal ganglia. Within the basal ganglia, however, coherence was predominantly directed from GP to STN and SNr. Together, these results highlight a lead role for the cortex in activity relationships with the basal ganglia, and further suggest that the effective direction of coupling between basal ganglia nuclei is dynamically organized according to brain state, with activity relationships involving the GP displaying the greatest capacity to change.

(Received 3 August 2004; accepted after revision 12 November 2004; first published online 18 November 2004)

Corresponding author P. Brown: Sobell Department of Motor Neuroscience and Movement Disorders, Institute of Neurology, Queen Square, London, WC1N 3BG, UK. Email: p.brown@ion.ucl.ac.uk

The basal ganglia (BG) are a group of subcortical brain nuclei intimately involved in movement and cognition. Much is known about the electrophysiology of the BG and their cortical inputs at the single-neurone level (see Boraud *et al.* 2002 for review), but the mechanisms by which the activities of large populations of cortical and BG neurones are coordinated remain obscure. It has been suggested by many authors that the coordination of activity at a population level is crucial to the function of the BG and related structures (Graybiel, 1995; Bergman *et al.* 1998; Stern *et al.* 1998; Brown, 2003). In cortical, thalamocortical and hippocampal circuits, there is emerging evidence that synchronized oscillatory activity is functionally important for orchestrating the activities of neuronal populations during behaviour (Steriade, 2000; Engel *et al.* 2001; Buzsáki & Draguhn, 2004). Within the cerebral cortex, local field potential (LFP) recordings provide a useful measure of the synchronized sub- and supra-threshold activities of local neuronal populations (Hubbard *et al.* 1969; Mitzdorf,

1985), and it is likely that LFPs recorded in the basal ganglia may afford similar information (Goto & O'Donnell, 2001; Levy *et al.* 2002; Courtemanche *et al.* 2003; Berke *et al.* 2004; Goldberg *et al.* 2004; Magill *et al.* 2004a,b). Recordings of LFPs from the BG of patients implanted with electrodes for the treatment of Parkinson's disease have confirmed strong synchronization of oscillatory population activity between STN and GP (Brown *et al.* 2001; Cassidy *et al.* 2002; Williams *et al.* 2002). Studies in patients have also shown that oscillations in the BG are often coherent with those in the cerebral cortex (Marsden *et al.* 2001; Cassidy *et al.* 2002; Williams *et al.* 2002).

The two major advantages of functional organization through synchronization are the potential for plasticity and the reconfiguration of neuronal associations according to brain state and behavioural task (Steriade, 2000; Engel *et al.* 2001). Previous studies in the urethane-anaesthetized rat have demonstrated brain state-dependent changes in

the coherent oscillatory activity between frontal ECoG and LFPs recorded from several BG nuclei, including the STN, GP and SNr (Magill *et al.* 2004b). During cortical slow-wave activity (SWA), which accompanies deep anaesthesia and is similar to activity observed during natural sleep, the coherence between ECoG and LFPs was largely confined to slow (< 2 Hz) and spindle-frequency (7–12 Hz) oscillations. During episodes of sensory stimulation-evoked ‘global activation’, which contain patterns of activity that are more analogous to those observed during the awake, behaving state, coherence was mostly restricted to high-frequency oscillations (15–60 Hz). Activities in STN, GP and SNr were temporally coupled to cortical activity in distinct ‘loops’ of coherence that were robustly and dynamically organized (Magill *et al.* 2004b). Thus, in keeping with the idea that synchronization of activity at the population level is an important feature of the functional organization of cortico-basal ganglia circuits, distinct functional loops exist within these circuits and these loops are reconfigured according to brain state. The critical questions therefore arise as to what is the effective direction of transmission of coherent oscillatory activity and whether this direction is also dynamic, changing with brain state.

Coherence provides a frequency-domain measure of the linear phase and amplitude relationships between two signals. It captures both the zero time-lag synchronization implicit in the generation of robust LFP oscillations by a local population of neurones, and the synchronization of processes with non-zero, but fixed, time lags, as may occur when, for example, there are significant conduction delays between synchronized populations of neurones. In the latter instance, however, coherence *per se* gives no information about the ‘effective direction of coupling’ between synchronized populations of neurones, i.e. which population activity leads in time. The most parsimonious explanation for such a relationship between two coherent population activities is that the leading population actually drives the lagging population of neurones. However, this may not be the only explanation for such a relationship (see Methods and Discussion), and hence, we use the term ‘effective direction of coupling’ to describe a pattern of temporal relationships rather than a unique state of connectivity. One measure, closely related to coherence, commonly used to estimate the effective direction of coupling is the phase spectrum, which describes the phase, and hence, time-delay, between two coherent signals in a specific frequency band (Halliday *et al.* 1995). However, paradoxical phase estimates can arise when different coherent activities have overlapping frequency components. In these cases, the phase estimate is, in reality, a mixture of distinct phases, each of which is associated with a different coherent activity (Cassidy & Brown, 2003). A good example of this is the afferent and efferent couplings between cortex and muscle (Mima *et al.* 2001).

Mixtures of activities with different phase relationships are particularly likely in highly interconnected circuits, such as the cortico-basal ganglia loops.

The directed transfer function (DTF) provides an alternative method of assessing the effective direction of coupling between brain regions (Kaminski & Blinowska, 1991; Cassidy & Brown, 2003). Importantly, the DTF is able to separate coherent activities that have overlapping frequency components, but which differ in their phase relationships (Kaminski & Blinowska, 1991; Cassidy & Brown, 2003). Accordingly, the DTF can provide information about the effective direction of coupling of the predominant coherent activity. Here, we use the DTF to analyse the effective direction of coupling between different BG nuclei, and between these nuclei and the cortex, during two different brain states in the urethane-anaesthetized rat. The DTF results obtained in the present study, when taken in the context of those previously obtained from partial coherence analysis of data generated in the same animals under the same recording paradigm (Magill *et al.* 2004b), are used to elucidate further the functional organization of oscillatory population activity in these circuits.

Methods

Electrophysiological recordings and verification of recording sites

Techniques for the electrophysiological recordings, and the labelling and histological verification of recording sites have been previously reported in detail (Magill *et al.* 2004b). Experimental procedures were carried out on adult male Sprague-Dawley rats (Charles River, Margate, UK) and were conducted in accordance with the Animals (Scientific Procedures) Act 1986 (UK).

Electrophysiological recordings were made in 12 rats (200–320 g). Anaesthesia was induced with isoflurane (Isoflo, Schering-Plough Ltd, Welwyn Garden City, UK) and maintained with urethane (1.3 g kg⁻¹, i.p.; ethyl carbamate, Sigma, Poole, UK), and supplemental doses of ketamine (30 mg kg⁻¹, i.p.; Ketaset, Willows Francis, Crawley, UK) and xylazine (3 mg kg⁻¹, i.p.; Rompun, Bayer, Germany), as previously described (Magill *et al.* 2000, 2001, 2004b). Anaesthesia levels were assessed by examination of the ECoG, and by testing reflexes to a cutaneous pinch or gentle corneal stimulation. Electrocardiographic (ECG) activity and respiration rate were also monitored constantly to ensure the animals’ well being.

The ECoG was recorded via a 1 mm diameter steel screw juxtaposed to the dura mater above the right frontal cortex (AP: –4.5 mm, ML: –2.0 mm (Paxinos & Watson, 1986), which corresponds to the medial agranular field of the somatic sensorimotor cortex (Donoghue & Wise,

1982)) and referenced against an indifferent electrode placed adjacent to the temporal musculature. Raw ECoG was band-pass filtered (0.1–150 Hz, –3 dB limits) and amplified (2000×, NL104 preamplifier; Digitimer Ltd, Welwyn Garden City, UK) before acquisition. This and adjacent regions of cortex project to both striatum and STN, as demonstrated in anatomical and electrophysiological studies (Fujimoto & Kita, 1993; Smith *et al.* 1998; Kolomiets *et al.* 2003; Magill *et al.* 2004a).

Extracellular recordings of LFPs in the ipsilateral GP, STN and SNr were simultaneously made with glass electrodes (6–12 MΩ measured at 10 Hz *in situ*, tip diameters of 2.5–3.0 μm) that were filled with a 0.5 M NaCl solution containing 1.5% w/v Neurobiotin (Vector Laboratories, Peterborough, UK). Extracellular signals from the three electrodes were amplified (10×) through the active bridge circuits of two Axoprobe-1A amplifiers (Axon Instruments, Union City, CA, USA). The LFPs were recorded after further amplification (100×; NL-106 AC–DC Amplifier, Digitimer) and low-pass filtering (between d.c. and 150 Hz; NL125 filters, Digitimer). The glass electrodes were independently referenced via wires inserted into the skin at the top of the neck. HumBug units (Quest Scientific, Vancouver, Canada) were used in place of traditional ‘notch’ filters to eliminate mains noise or ‘hum’ at 50 Hz (Brown *et al.* 2002). Recordings of spontaneous activity typically lasted for 20–40 min.

Sensory stimulation and subsequent global activation were elicited by pinching the hindpaw for 15 s with serrated forceps that were driven by a standard pneumatic pressure, as previously described (Magill *et al.* 2004b). The animals did not exhibit either a marked change in ECG/respiration rates or a hindpaw withdrawal reflex in response to the pinch.

After the recording and stimulation sessions, all recording locations were marked by discrete, extracellular deposits of Neurobiotin (100 nA anodal current; 1 s (50%) duty cycle for 60 min; Magill *et al.* 2004b). Following perfusion–fixation, brains were sectioned and standard techniques were used to visualize the Neurobiotin deposits (Horikawa & Armstrong, 1991; Magill *et al.* 2001). The precise locations of all recording sites in the BG were histologically verified. The central and medial two-thirds of the GP, and all regions of STN and SNr were sampled in this study (see Fig. 1 in Magill *et al.* 2004b).

Data acquisition and analysis

All biopotentials were digitized on-line at 400 Hz with a PC running Spike2 acquisition and analysis software (version 4; Cambridge Electronic Design Ltd, Cambridge, UK). Data from the recording session were first scrutinized for ECG artefacts; data contaminated with ECG artefacts were rejected. Artefact-free data were then visually inspected

and epochs of robust cortical slow-wave activity or global activation were identified (Magill *et al.* 2004b).

The directed transfer function (DTF) investigates any possible asymmetry in the flow of coherent activity between regions (Kaminski & Blinowska, 1991). To this end, the multiple autoregressive (MAR) model that best described the signals coming from the two regions of interest was determined. The MAR methodology is essential for the DTF, as the DTF is built directly from the MAR coefficients. Following the procedure detailed in Cassidy & Brown (2002), a Bayesian methodology was applied to estimate the parameters of the autoregressive model. This approach is desirable in that it provides full probabilistic distributions for all of the model parameters. In addition, the complexity of the model (i.e. the most appropriate number of spectral peaks) is determined objectively and automatically based on the data supplied to the model. The Bayesian update equations for the MAR coefficients are similar in form to the standard maximum likelihood equations, but additionally incorporate a prior precision term, α , and are given by:

$$\hat{\Sigma} = (\Lambda \otimes XT X + \alpha I_k) - 1 \quad (1)$$

$$\hat{a} = \hat{\Sigma}(\Lambda \otimes XT X)a_{ml} \quad (2)$$

They are given by the normal distribution $N(a|\hat{a}, \hat{\Sigma})$; Λ is the noise precision, X is a matrix containing the regressors, a_{ml} is the usual maximum likelihood solution for the coefficients, I_k is the identity matrix and $k = pd^2$, where p is the model order and d is the number of channels, while \otimes denotes the Kronecker product. For further details, the reader is referred to Cassidy & Brown (2002, 2003).

The autoregressive coefficients can be used to construct a bounded, normalized measure (the DTF) that provides information on the effective direction of coupling. The off-diagonal MAR coefficients indicate the temporal coupling between one site and another, and (depending on whether they are upper or lower off-diagonal) the direction of that coupling. By squaring and normalizing the MAR coefficients, the DTF is obtained, as described by Kaminski & Blinowska (1991).

Where the DTF of coherent activity at two recording sites was symmetrical, no one ‘effective direction of coupling’ predominated, either because phase delays of mixed coherent activities were balanced or there was genuine synchronization with zero phase (and time) difference (see Cassidy & Brown, 2003 and Fig. 1A and B). Where the DTF of coherent activity at two recording sites was asymmetrical, the ‘effective direction of coupling’ predominated in one direction and coherent activity or activities in one population of neurones tended to lead in time (Fig. 1). It should be noted, however, that an asymmetrical DTF does not necessarily imply a direct connection between the two areas in which activity was recorded. Thus, information can be transferred indirectly

between recorded structures, via one or more unrecorded structures, or indeed, activity in both recorded structures may be driven by a third unrecorded structure (Fig. 1C and D). The relative time delays between different structures and intermediate relays may also influence the effective direction of coherent activity (Fig. 1D). As such, the interpretation of the DTF has to be informed by evidence of anatomical connectivity and/or other sources of evidence for functional connectivity (see Discussion).

Recordings from 10 animals were suitable for DTF analysis. Data from two animals previously used for fast Fourier transform (FFT)-based spectral analysis (Magill *et al.* 2004b) were excluded due to ambiguity in the selection of the MAR model order. For each animal, data were organized so as to consist of separate pairs of recording sites. All the pairs were modelled and analysed separately. This bivariate approach gave a more

detailed spectral picture than the simultaneous analysis of the multivariate data. Selection of the model order for each pairing is discussed above. Separate analyses were performed on recordings made during slow-wave activity and global activation in all animals.

An 80 s epoch of the cortical and BG activity present during deep anaesthesia with robust cortical slow-wave activity (described in detail in Magill *et al.* 2004b) was selected for each animal. To better model low-frequency activity, these data segments were down-sampled to 20 Hz (after appropriate low-pass filtering to avoid aliasing). The fact that activity at frequencies of < 10 Hz dominated these data segments had already been established using FFT methods (see Magill *et al.* 2004b). For cortex–basal ganglia pairings, statistical analysis was performed on frequencies between 0.1 Hz and 2 Hz, a range that encompasses the bulk of the coherent activity present in this brain state, as verified by both DTF (see Fig. 3A–C), and FFT methods (Magill *et al.* 2004b). Statistical analysis for basal ganglia–basal ganglia pairings during slow-wave activity were analysed using a smaller range (0.1–1 Hz) because the DTFs displayed narrower peaks as compared to the DTFs of cortical–basal ganglia pairings (see Fig. 3D–F). To investigate activity present during sensory stimulation-evoked global activation, three data segments (20 s each) recorded during (15 s) and immediately after (5 s) hindpaw pinches were analysed separately and then averaged to give single values for each animal. Before DTF analysis, these files were down-sampled to 200 Hz (after appropriate low-pass filtering to avoid aliasing) to detect coherence below 100 Hz, and statistical analysis was performed on values between 15 Hz and 60 Hz. Again, this frequency range contains much of the coherent activity present in cortex and BG during global activation (Magill *et al.* 2004b). Standard coherence analysis was also performed using the same autoregressive model as that used for the DTF on all channel pairings, in both brain states, to confirm that there was significant coherent activity in these bands. For each frequency range (0.1–2 Hz, 0.1–1 Hz and 15–60 Hz), the DTF values for each direction of each recording site pairing were averaged in each animal. Student's paired *t* test was then performed on all pairings to determine whether coherence was consistently greater in one direction across all 10 animals.

The above analyses investigated the effective direction of coupling in averaged data. Time-evolving DTF analysis was used to confirm that any changes in effective direction of coupling between structures associated with brain state could be seen in a single record. Time-evolving DTF plots (see Fig. 5) were constructed using DTF coherence values calculated in consecutive 10 s windows (with 5 s overlap). For each window, the coherence values in one direction (e.g. effective direction of coupling from GP to STN) were made negative and summed with those in the

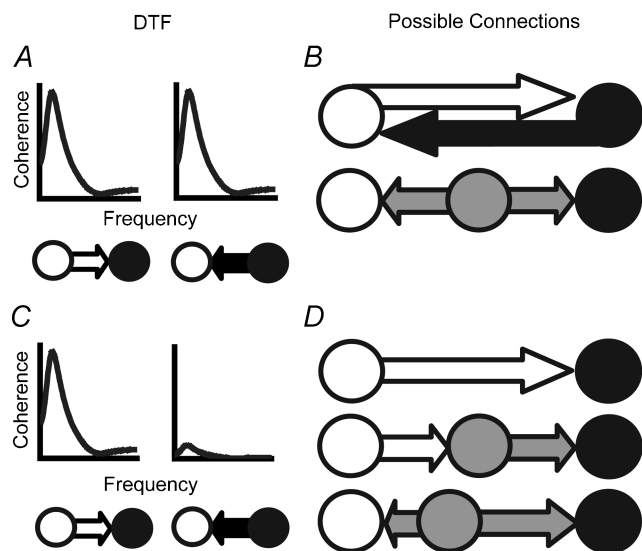


Figure 1. Possible interpretations of symmetrical and asymmetrical directed transfer functions of coherent activity in two recording sites

A and B, symmetrical DTF and possible underlying connections. A, the two DTF graphs are identical, indicating that the net flow of coherent activity between recording sites 1 (white circle) and 2 (black circle) is equal. Arrows represent direction of coherent activity detected by DTF analysis. B, identical DTF graphs could be produced by an equal and direct flow of coherent activity between the two recording sites (top). Alternatively, information could be transferred indirectly between recording sites from a third connecting structure (grey; not recorded). C and D, asymmetrical DTF and possible underlying connections. C, dissimilar DTF graphs show that the flow of coherent activity from site 1 to site 2 is significantly greater than the flow from site 2 to site 1. D, asymmetries could indicate that activity at site 2 is directly driven by activity at site 1 (top). This dependence, however, might not be due to a direct influence, but may involve feed-forward propagation via a third site (middle). Alternatively, coherent activity at recording sites may be driven by a third site (bottom). If the latency of propagation from the third site to recording site 1 is shorter than the latency to site 2, then site 1 will have a larger DTF and, thus, will apparently drive site 2 (bottom).

opposite direction (e.g. effective direction of coupling from STN to GP). This resulted in a single coherence value in each frequency bin, with the direction of asymmetry represented by the sign (e.g. negative when effective direction of coupling is from GP to STN, and positive when effective direction of coupling is from STN to GP), and the magnitude of that asymmetry represented by the coherence value (e.g. a value of +1.0 would represent: (1) all activity in that frequency bin being completely coherent; and (2) coherent activity being completely asymmetrical and all coupling is in the direction of STN to GP). Coherence at low frequencies (30 Hz sampling rate, 0.3 Hz bins) and high frequencies (100 Hz sampling rate, 1 Hz bins) was analysed separately at sampling rates that maximized detection of these activities. In this case, analysis of low-frequency activity was performed using a 30 Hz sampling rate (rather than 20 Hz as in other analyses) to increase data points within the 10 s windows. The frequency bins displayed (Fig. 5) have been chosen to approximate those used in the main statistical analysis (see above).

Results

DTF of activity present during robust cortical slow-wave activity

We have previously shown that during the robust slow-wave activity prevalent under urethane anaesthesia, oscillatory activity in frontal ECoG and basal ganglia LFPs is dominated by low-frequency rhythms at ~ 1 Hz (see Magill *et al.* 2004b and Fig. 2). Analysis of the standard coherence between cortex and basal ganglia LFPs, and between basal ganglia LFPs themselves, confirmed the presence of strongly coupled activity at low frequencies across animals, with lower 95% confidence levels that were well above zero (see Table 1). Directed transfer function analyses of the coherent activity present in the cortex and basal ganglia during this brain state were performed to detect asymmetries in the directed coherence at low frequencies. The highest directed coherence between activity in cortex and basal ganglia was seen between 0.1 and 2 Hz (see Fig. 3A–C). The mean coherence at 0.1–2 Hz in the DTFs of the basal ganglia recording sites was used to assess the effective direction of coupling to, and from, the cortex. Coherence between cortex and basal ganglia

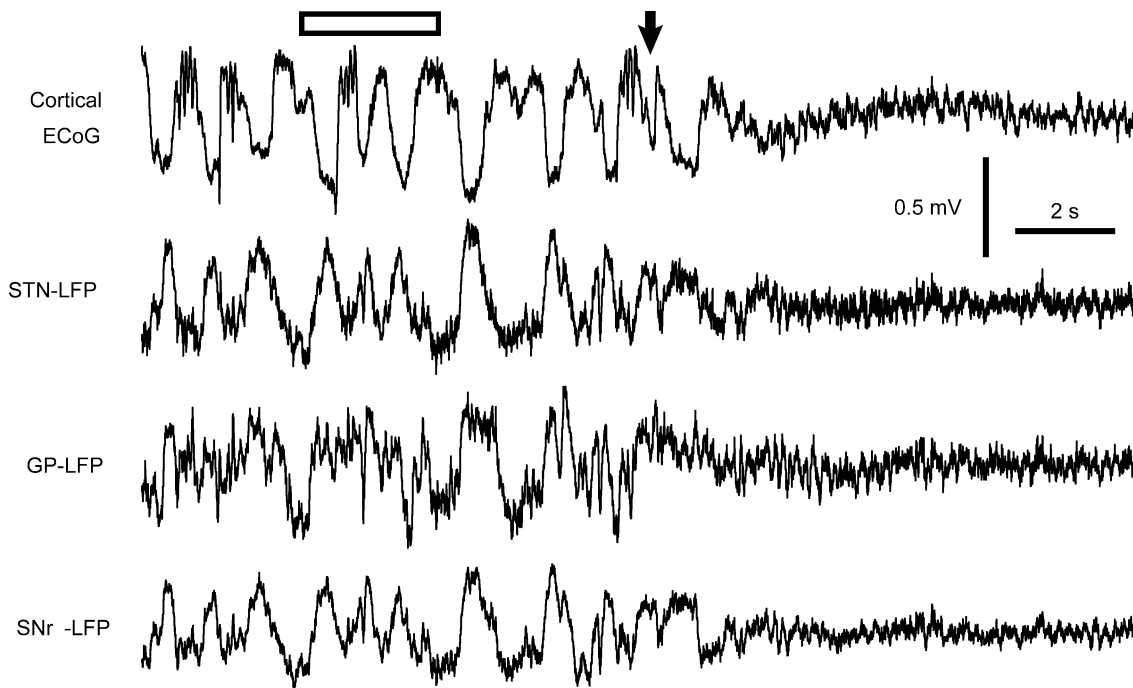


Figure 2. Simultaneous recordings of ECoG of frontal cortex and local field potentials in the basal ganglia during slow-wave activity and global activation

The ECoG was dominated by a slow oscillation (~ 1 Hz) of large amplitude during spontaneous slow-wave activity. Local field potentials simultaneously recorded in STN, GP and SNr displayed similar oscillatory phenomena, but with reversed polarities compared to cortical activity. Note that the LFP in GP did not reflect the cortical slow oscillation as faithfully as did LFPs in STN and SNr (see epoch under open bar). Global activation of the forebrain following pinch onset (arrow) was exemplified by a loss of slow-wave oscillations in the ECoG, and a shift to oscillatory activity of smaller amplitude and higher frequency. Local field potentials in GP, STN and SNr displayed similar shifts in oscillatory phenomena. Calibration bars apply to all panels.

Table 1. Differences in the effective direction of coherent activity recorded in the cortex and basal ganglia during slow-wave activity

| Pairings of recording sites | ECoG/STN (0.1–2 Hz) | ECoG/GP (0.1–2 Hz) | ECoG/SNr (0.1–2 Hz) | STN/GP (0.1–1 Hz) | STN/SNr (0.1–1 Hz) | GP/SNr (0.1–1 Hz) |
|--------------------------------|------------------------|-----------------------|------------------------|----------------------|-----------------------|----------------------|
| Transformed standard coherence | 0.86 ± 0.13 | 0.60 ± 0.12 | 0.88 ± 0.13 | 1.25 ± 0.26 | 1.34 ± 0.24 | 1.58 ± 0.26 |
| Direction | ECoG to STN | ECoG to GP | ECoG to SNr | STN to GP | STN to SNr | GP to SNr |
| Transformed directed coherence | 0.63 ± 0.14 | 0.68 ± 0.17 | 0.68 ± 0.13 | 1.36 ± 0.41 | 0.43 ± 0.06 | 0.52 ± 0.18 |
| Direction | STN to ECoG | GP to ECoG | SNr to ECoG | GP to STN | SNr to STN | SNr to GP |
| Transformed directed coherence | 0.33 ± 0.13 | 0.16 ± 0.06 | 0.30 ± 0.09 | 0.42 ± 0.09 | 0.81 ± 0.24 | 1.20 ± 0.47 |
| Paired <i>t</i> test | <i>P</i> < 0.04 | <i>P</i> < 0.001 | <i>P</i> < 0.01 | <i>P</i> < 0.01 | <i>P</i> < 0.05 | <i>P</i> < 0.01 |
| Lead structure | ECoG | ECoG | ECoG | STN | SNr | SNr |

Transformed standard coherence and Transformed directed coherence are shown ± 95% confidence limits (CL). ECoG, electrocorticogram; GP, globus pallidus; SNr, substantia nigra *pars reticulata*; STN, subthalamic nucleus. All standard and directed coherence values have been Fisher transformed. Significance for confidence limits (CL) of the mean and paired *t* tests were set at *P* ≤ 0.05. For *t* test results, the leading structures where the DTF is asymmetric are shown in bold.

was asymmetrical, with significantly more low-frequency coherence being directed from cortex to STN, GP and SNr than vice versa (Fig. 3A–C and Table 1). The highest coherence in all pairings between STN, GP and SNr was at ~1 Hz, but there was also coherence at slightly higher frequencies, which was most clearly seen in the DTF between STN and SNr (Fig. 3D–F). The DTF between basal ganglia sites was narrower than that between cortex and basal ganglia sites, so statistical analysis was performed on values between 0.1 and 1 Hz (see Fig. 3D–F and Table 1). Directed coherence in this range between all basal ganglia pairings was asymmetrical. There was significantly more coherence directed from SNr to both STN and GP, and from STN to GP (Table 1).

DTF of activity present during global activation

Recordings of activity present during global activation were analysed specifically to detect directed coherence at higher frequencies (15–60 Hz), i.e. the frequency band containing the dominant coherent activities as previously recorded in anaesthetized rats (see Magill *et al.* 2004b and Fig. 2) and showing significant standard coherence between cortex and basal ganglia LFPs and between basal ganglia LFPs themselves (see Table 2). Some coherent low-frequency activity (< 5 Hz) was still present from all recording site pairings, although this was reduced relative to that present in robust slow-wave activity, as previously described (Magill *et al.* 2004b). Coherence spectra derived from some animals had clear peaks at higher frequencies, particularly at around 20 Hz and 50 Hz. However, such clear peaks were not consistently found, such that coherence was best described as ‘broadband’ when considered across the whole experimental population (Fig. 4). Nevertheless, coherence at 15–60 Hz was significantly higher during global activation compared to slow-wave activity (data not shown, but see Magill *et al.* 2004b). In all but one pairing, that between SNr and STN, the DTFs showed at

least some degree of asymmetry (Fig. 4A–F). Cortico-basal ganglia relationships at these high frequencies were similar to those at low frequencies (compare Figs 3 and 4), with significantly more coherence directed from cortex to all the basal ganglia sites (Fig. 4A–C and Table 2). In contrast, the relationships between different basal ganglia sites were profoundly different from those evident during slow-wave activity. There was significantly more high-frequency coherence directed from GP to both STN and SNr (Fig. 4D and E, Table 2) than vice versa, while the coherence between STN and SNr across animals became symmetrical (Fig. 4F). Global activation thus produced a selective reversal in the effective direction of coupling in those pairings involving GP.

Time-evolving DTF analysis was used to confirm that the changes in the direction of coherence between STN and GP associated with global activation could be seen in a single record (Fig. 5). During spontaneous slow-wave activity, as assessed from the ECoG, periods of asymmetrical low-frequency coherence, in which the effective direction of coupling from STN to GP dominated, were interspersed with periods of asymmetrical high-frequency coherence, in which the effective direction of coupling from GP to STN dominated. During and after the induction of global activation by hindpaw pinch, high-frequency coherence directed from GP to STN increased in magnitude and became more sustained, while the low-frequency coherence reversed its asymmetrical pattern so that most activity was directed from GP to STN rather than from STN to GP. Thus, the highly dynamic relationship between STN and GP could be observed in single recording sessions.

Discussion

The main findings of the present study are that the effective direction of coherent oscillatory activity in the cerebral cortex and basal ganglia is predominantly from the cortex to the basal ganglia during two different brain

states, slow-wave activity and global activation. However, and in stark contrast, the effective directions of coherent oscillatory activity in the nuclei of the basal ganglia are dynamic and dependent on brain state.

Coherent population oscillations in cortico-basal ganglia circuits are predominantly directed from cortex during slow-wave activity and global activation

In both brain states investigated, the effective direction of coupling was from cortex to basal ganglia rather than *vice versa*, at least as far as activity in the predominant frequency bands was concerned (Fig. 6). As with cross

correlation or phase analysis, there is no assurance that directed coherence from one recording site to another indicates a direct connection between the two sites. However, it is known, at the single-neurone level, that the slow oscillation (at ~ 1 Hz) present in the cortex during anaesthesia drives low-frequency oscillations in the STN, via direct connections, and, to a lesser extent, GP and SNr via indirect routes (Magill *et al.* 2000, 2001, 2004b). The DTF analysis presented here suggests that this is also true of local field potentials.

Cortico-basal ganglia connections are not functionally homogeneous. Previous FFT analyses have shown that coherent cortical SWA is shared more strongly between STN and SNr than GP (Magill *et al.* 2004b). The coherence

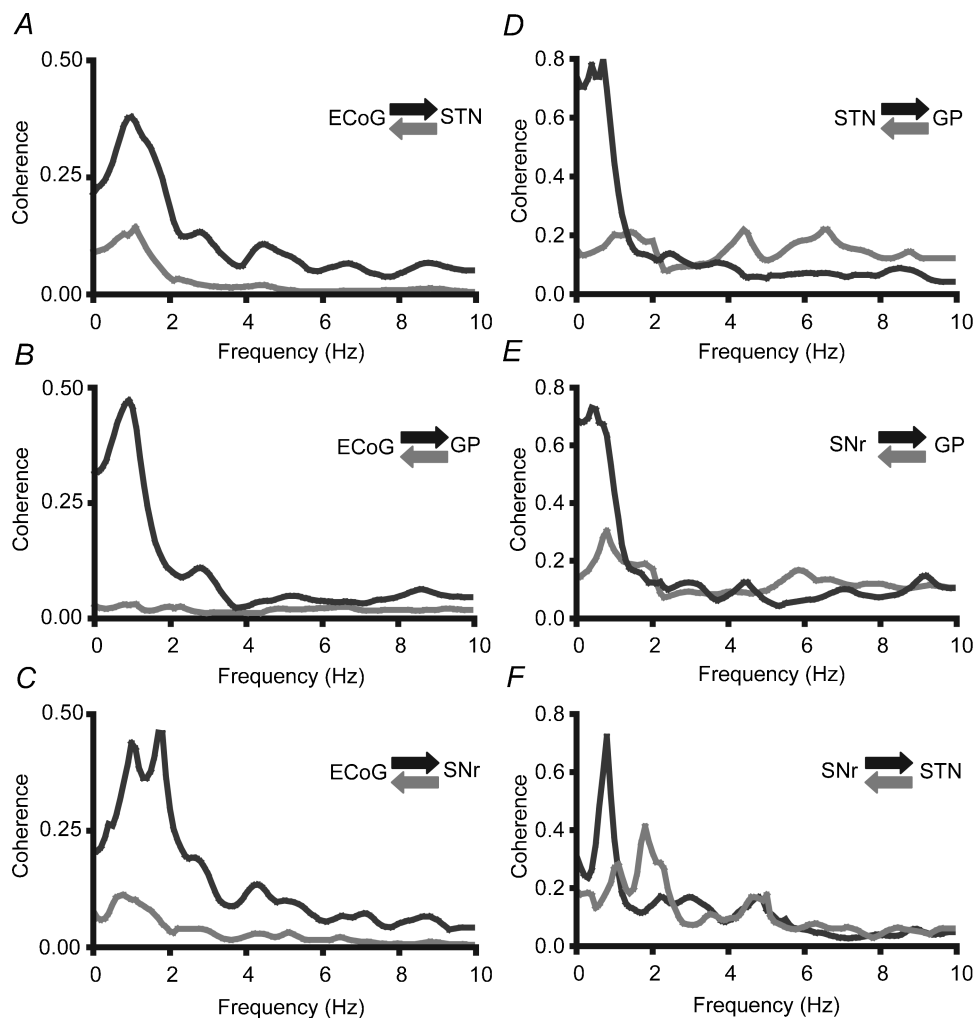


Figure 3. Directed transfer function analysis of local field potentials recorded in cortex and basal ganglia during robust slow-wave activity

Plots were constructed using the mean coherence in each direction for each individual recording site pairing ($n = 10$ animals). Coherence in all pairings was confined mostly to 0.1–2 Hz and, in nearly all cases, peaked at around 1 Hz. A–C, coherence between cortex (ECoG) and all three basal ganglia recording sites (STN, GP and SNr) was asymmetrical, with the effective direction of coherent oscillatory activity being from cortex to the basal ganglia (black) rather than vice versa (grey). D, coherence between STN and GP was asymmetrical, with the effective direction of coherent oscillatory activity at ~ 1 Hz being from STN to GP (black) rather than vice versa (grey). E and F, coherence between SNr and GP and between SNr and STN was asymmetrical, with more coherent activity being directed from SNr. Note different y-axis scales for cortex–basal ganglia and basal ganglia–basal ganglia pairings.

Table 2. Differences in the effective direction of coherent activity recorded in the cortex and basal ganglia during global activation

| Pairings of recording sites (15–60 Hz) | ECoG/STN | ECoG/GP | ECoG/SNr | STN/GP | STN/SNr | GP/SNr |
|--|------------------|-----------------|-----------------|------------------|-------------|------------------|
| Transformed standard coherence | 0.34 ± 0.06 | 0.44 ± 0.07 | 0.26 ± 0.04 | 0.71 ± 0.10 | 0.63 ± 0.07 | 0.57 ± 0.08 |
| Direction | ECoG to STN | ECoG to GP | ECoG to SNr | STN to GP | STN to SNr | GP to SNr |
| Transformed directed coherence | 0.30 ± 0.07 | 0.32 ± 0.09 | 0.27 ± 0.08 | 0.15 ± 0.04 | 0.25 ± 0.06 | 0.30 ± 0.05 |
| Direction | STN to ECoG | GP to ECoG | SNr to ECoG | GP to STN | SNr to STN | SNr to GP |
| Transformed directed coherence | 0.08 ± 0.03 | 0.14 ± 0.04 | 0.10 ± 0.04 | 0.37 ± 0.07 | 0.25 ± 0.07 | 0.13 ± 0.03 |
| Paired <i>t</i> test | <i>P</i> < 0.001 | <i>P</i> < 0.02 | <i>P</i> < 0.02 | <i>P</i> < 0.001 | NS | <i>P</i> < 0.001 |
| Lead structure | ECoG | ECoG | ECoG | GP | | GP |

Transformed standard coherence and transformed directed coherence are shown ± 95% confidence limits (CL). ECoG, electrocorticogram; GP, globus pallidus; SNr, substantia nigra *pars reticulata*; STN, subthalamic nucleus. All standard and directed coherence values have been Fisher transformed. Significance for confidence limits (CL) of the mean and paired *t* tests were set at *P* ≤ 0.05. For *t* test results, the leading structures where the DTF is asymmetric are shown in bold. NS, not significant.

between cortex and GP may therefore reflect a relatively independent loop of activity during SWA. The reasons for this are not known. Given that LFPs may largely reflect synaptic input (for reviews, see Hubbard *et al.* 1969; Mitzdorf, 1985), an explanation for independent loops of coherent activity could be that the GP is more sensitive to slow oscillatory input from striatal neurones, which are also entrained by the cortical slow oscillation (Stern *et al.* 1997; Tseng *et al.* 2001; Kasanetz *et al.* 2002). In contrast, the STN, which is tightly coupled with SNr, is most likely driven directly by the cortico-subthalamic pathway (Magill *et al.* 2001, 2004b) and, thus, is relatively independent of the GP in this brain state (Magill *et al.* 2000; Urbain *et al.* 2000). Irrespective of the pathway(s) subserving temporal coupling between cortex and GP or cortex and SNr, i.e. trans-subthalamic and/or trans-striatal pathways, the fact remains that the cortex provides the major driving force for low-frequency oscillations in LFPs recorded from these basal ganglia nuclei. That said, it should be noted that a small proportion of coherent activity was consistently directed from the basal ganglia to the cortex, which may reflect the looping architecture of the cortico-basal ganglia circuits (Alexander & Crutcher, 1990; Haber, 2003; Kelly & Strick, 2004).

Sensory stimulation led to a suppression of slow-wave activity in the ECoG, i.e. global activation, and an increase in coherence between the cortex and basal ganglia at higher frequencies, as previously reported (Magill *et al.* 2004b). From the present DTF results, however, it is clear that the effective direction of coherent oscillatory activity is unchanged during global activation, being principally driven by the cortex.

The effective direction of coherent population oscillations in the basal ganglia is dependent on brain state and recording location

Two questions that remain are why the effective direction and sharing of coherent oscillatory activity between basal ganglia nuclei changes with brain state, and why this phenomenon might be of importance. The interpretation

of activity relationships within the basal ganglia is more challenging given the highly interconnected nature of the constituent neuronal networks (Smith *et al.* 1998; Bolam *et al.* 2000). This is well illustrated by the directed coherence between STN and SNr. Partial coherence analysis suggests that the oscillatory activities in STN and SNr that are coherent with cortical oscillations are bound together tightly in a single functional axis (Magill *et al.* 2004b). Given that the anatomical connections between STN and SNr are thought to be limited to projections from the former only (Smith *et al.* 1998), it might be expected that the DTFs would be asymmetrical, with coherence being directed primarily from STN to SNr. During global activation, however, coherent activity between the two sites was found to be symmetrical. There could be several reasons why this was the case in the present experiments. The first possibility is that volume conduction between the two electrodes led to spurious symmetrical coupling. If this were the case, then the DTFs would be expected to be symmetrical for all individual subjects. However, the DTFs derived from individual animals were often asymmetrical between STN and SNr; the direction of the asymmetry was inconsistent across animals, thereby leading to apparent symmetry in the population average. Moreover, volume conduction would have been expected to lead to symmetrical directed coherence regardless of brain state, and this was not so. Alternatively, the inconsistent asymmetry of the DTFs may have been a reflection of two functionally distinct axes of coupling between STN and SNr. However, because data were necessarily pooled for statistical analysis, the existence and significance of such axes remain to be verified. The asymmetrical nature of individual DTFs raises the second possibility that the STN and SNr were being driven by a third site with equal or unequal time delays, which, in turn, would depend on recording location and the topography of underlying neuronal circuits, thus creating inconsistencies in direction (see Fig. 1D). An obvious candidate for a third site would be GP because the effective direction of coherent oscillatory activity from GP to both structures dominated over that in the reverse direction during global

activation (Fig. 6B). Of course, the demonstration of a direct projection from SNr to STN might help explain the symmetry apparent in the mean DTFs and, in fact, preliminary anatomical studies suggest that this projection may exist (J. Deniau, personal communication). Finally, it is also possible that the DTF estimates may have become unreliable due to the small conduction delays between STN and SNr (Cassidy & Brown, 2003).

A surprising result was also seen during slow-wave activity, when there was significantly more coherent activity directed from SNr to STN. This again raises the possibility of a direct connection from SNr to STN, preferentially showing activity of low frequency during slow-wave activity. Note however, that there are two peaks

in the DTF of activity between SNr and STN. The DTF over 0.1–1 Hz showed a predominant effective direction of coherent oscillatory activity from SNr to STN, but the DTF at a slightly higher frequency of around 2 Hz demonstrated the expected direction from STN (Fig. 3F). Of course, we cannot rule out the possibility that a third (unrecorded) site provides an important functional interface between SNr and STN (see Fig. 1D). Two key contenders for such an interface are the intralaminar thalamic nuclei and the pedunculopontine tegmental nucleus; both of these brain areas receive extensive inputs from SNr and in turn project to STN (Mena-Segovia *et al.* 2004; Smith *et al.* 2004). Overall, the pattern of directed coherence between basal ganglia sites during slow-wave activity suggests that the full

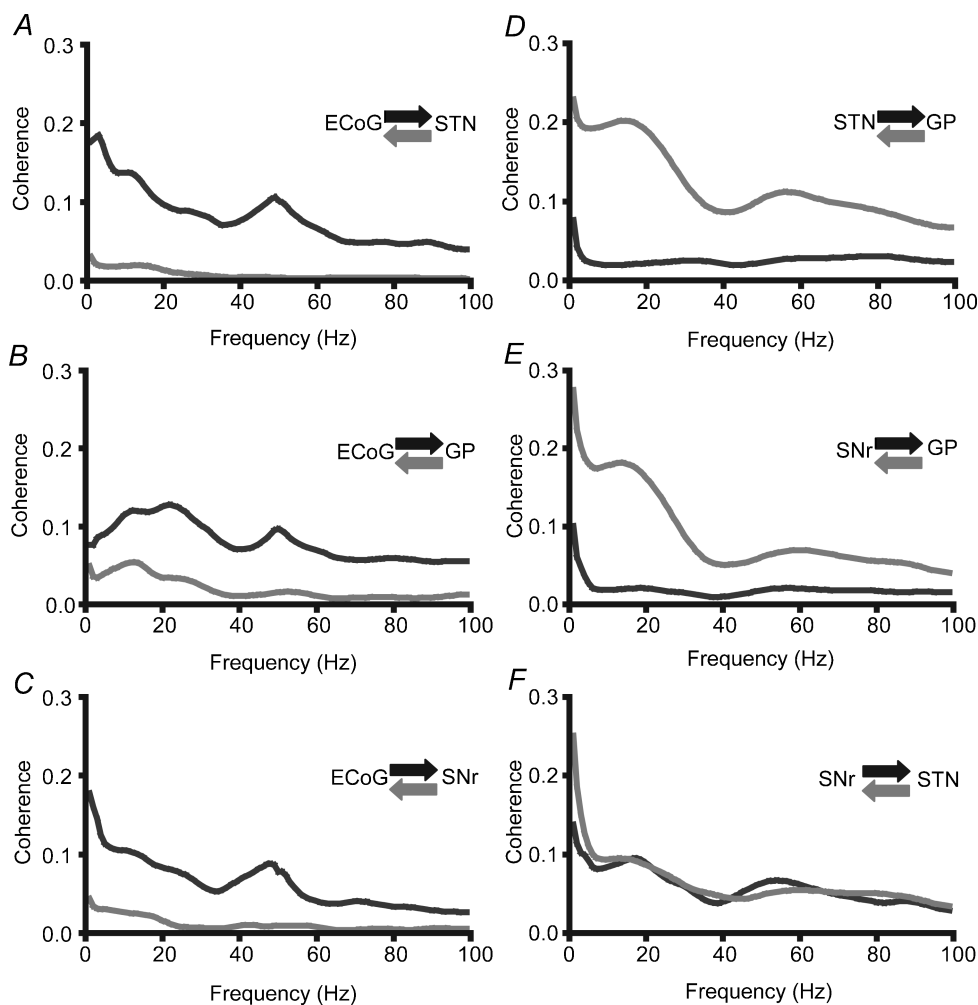


Figure 4. Directed transfer function analysis of local field potentials recorded in cortex and basal ganglia during global activation

Plots were constructed using the mean coherence in each direction for each individual recording site pairing ($n = 10$ animals; same as shown in Fig. 3). Coherence was seen over a broad range of frequencies between 15 and 60 Hz. A–C, coherence between cortex (ECoG) and the basal ganglia (STN, GP and SNr) was asymmetrical, with the effective direction of coherent oscillatory activity being from cortex to the basal ganglia (black) rather than vice versa (grey). D and E, directed coherence at 15–60 Hz was significantly higher from GP to both STN and SNr (grey) than from either STN or SNr back to GP (black). F, in contrast, STN and SNr had symmetrical coherence at these high frequencies. Note different y-axis scale as compared to Fig. 3.

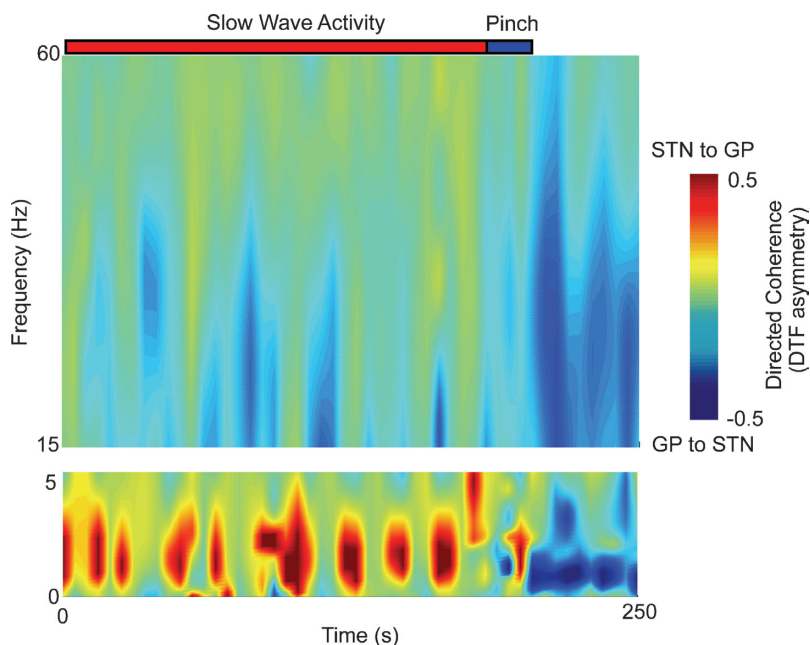


Figure 5. Time-evolving directed transfer function analysis of local field potentials recorded in subthalamic nucleus and globus pallidus

Plot was constructed from data acquired during a single contiguous recording. Low and high frequencies have been analysed at different sampling rates and are therefore separated. Two frequency blocks have been chosen to show the dominant activities most clearly: 0–5 Hz and 15–60 Hz. The colour scale represents the relative asymmetry of coherent activity in either direction. During spontaneous slow-wave activity, periods of asymmetrical low-frequency coherence, with more activity directed from STN to GP, were interspersed with periods of asymmetrical high-frequency coherence, with more activity directed from GP to STN. During and after the induction of global activation by a 15 s hindpaw pinch, high-frequency coherence directed from GP to STN increased and became more sustained, while the low-frequency coherence reversed direction so that most activity was directed from GP to STN rather than from STN to GP.

complexity and subtlety of their interconnections have not yet been fully established.

The most dramatic changes in the effective direction of information flow to accompany shifts in brain state were seen in paired recordings involving GP. During SWA, directed coherence between STN and GP was asymmetrical, with flow mostly going from STN to GP. Low-frequency oscillations in STN are known to be driven by cortex and are clearly seen at the levels of units, pairs of units, and LFPs (Magill *et al.* 2000, 2001, 2004*b*). Local field potentials recorded in GP are less strongly coupled to

the cortical oscillations at low frequencies, in agreement with the finding that similar oscillations do not manifest readily in single unit recordings (Magill *et al.* 2004*b*). Thus, low-frequency oscillations in STN are unlikely to be driven by GP (also see Magill *et al.* 2000; Urbain *et al.* 2000). Furthermore, standard coherence analysis has suggested that temporal coupling of cortex with STN (and SNr) during SWA is not shared with GP, which may rely more heavily on striatal inputs (Magill *et al.* 2004*b*). As the cortico-subthalamic pathway is considerably faster than the cortico-striato-pallidal pathway in transmitting cortical information to the basal ganglia (Nambu *et al.* 2000, 2002; Magill *et al.* 2004*a*), it is possible that the asymmetry between STN and GP could be due to the time difference between these input pathways (Fig. 1*D*).

During global activation, the effective direction of coherent oscillatory activity was predominantly from both cortex and GP to STN and SNr, suggesting that subthalamic and nigral LFP oscillations are partly derived from the cortex via the pallidum. Given that the STN and GP (or the external segment of GP in primates) are reciprocally connected (Shink *et al.* 1996; Bevan *et al.* 2002), the GP may play an important role in driving high-frequency oscillatory activity in STN. Consistent with the above, coherence and partial coherence analyses have shown that during global activation, all high-frequency coherent activity between cortex and STN (and SNr) is shared with that between cortex and GP (Magill *et al.* 2004*b*). In addition, the synchronous responses of STN neurones to cortical stimulation are partly due to interconnections with both cortex and GP (Magill *et al.* 2004*a*). The axons of GP neurones collateralize locally, as well as in STN and SNr (Kita & Kitai, 1994; Bevan *et al.* 1998; Sato *et al.* 2000). Furthermore, up to 40% of

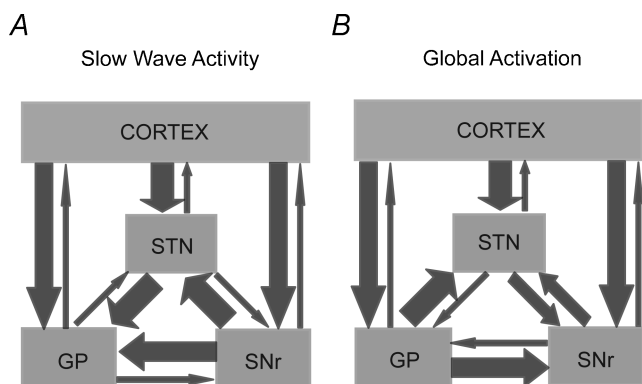


Figure 6. Summary diagrams showing directions of coherent activity present in cortico-basal ganglia circuits during slow-wave activity and global activation

Predominant coherence was found at 0.1–2 Hz during slow-wave activity (A) and at 15–60 Hz during global activation (B). Pairs of arrows represent the effective direction of coherence between recording sites. When one arrow is thicker, the effective direction of coherence was significantly larger in that direction. Identical arrows between sites indicate that there was no significant asymmetry in the directed coherence. Note that the relationships between the basal ganglia sites are dynamic and dependent on brain state.

GP cells also project to the striatum (Bevan *et al.* 1998; Sato *et al.* 2000; Kita & Kita, 2001). The GP is therefore in an ideal position to synchronize activity across the whole of the basal ganglia neuronal networks, and, indeed, the present results suggest that this may in fact occur, particularly at the higher frequencies predominating in the activated brain state. Thus, under these circumstances, GP could provide a critical link between, or interface for, the cortico-subthalamic and cortico-striatal input pathways (Nambu *et al.* 2002).

What might underlie the shift in the impact of the cortico-striatal pathway during global activation? It is well documented that the 'up states' of striatal projection neurones, which need to be achieved before firing can occur, are entrained by cortical slow rhythms during anaesthesia (Stern *et al.* 1997, 1998; Mahon *et al.* 2001; Goto & O'Donnell, 2001; Kasanetz *et al.* 2002). Yet, striatal neurones discharge relatively few spikes during SWA because they also spend a significant amount of time in the 'down state' (Mahon *et al.* 2001; Tseng *et al.* 2001; Kasanetz *et al.* 2002). During global activation, however, striatal projection cells assume a prolonged up state, which increases the likelihood of striatal unit firing (Murer *et al.* 2002) and may sometimes result in increased activity (Chudler *et al.* 1993; West, 1998; but see Kasanetz *et al.* 2002). This will in turn increase the efficacy of the cortico-striato-pallidal pathway. The finding that coherent activity between GP and STN is led by GP during cortical activation, but not during slow-wave activity, is strongly suggestive of a switch in the relative dominance of the cortico-subthalamic and cortico-striatal-pallidal pathways according to the ongoing brain state. The functional state of the striatum, which provides the densest input to GP (Smith *et al.* 1998; Bolam *et al.* 2000), may partly explain this switch. Bidirectional coherence at high frequencies between STN and SNr could also be due to both structures receiving pallidal input (see above). This explanation is consistent with recent hypotheses about the functional role of the two cortico-basal ganglia pathways in the active brain (Nambu *et al.* 2002; Kolomiets *et al.* 2003).

Role of synchronized population activity in cortico-basal ganglia circuits

Our results establish the principle that synchronous population activity within cortico-basal ganglia circuits can be dynamic, consistent with a functional role for synchronization of activity at different frequencies in large-scale integrative processes during sleep and wakefulness. Synchronization of activity, however fleeting, potentially facilitates the appropriate selection, assembly and disassembly of neural networks, according to processing demands, and may be an important organizational principle in cortico-basal ganglia circuits

(Graybiel, 1995; Bar-Gad *et al.* 2003). In line with this, oscillatory LFPs recorded in the striatum of awake monkeys and rats (Courtemanche *et al.* 2003; Berke *et al.* 2004), the STN of alert rats (Brown *et al.* 2002), and the STN of parkinsonian patients (Cassidy *et al.* 2002a; Williams *et al.* 2003; Kühn *et al.* 2004) are modulated in a task-dependent manner. However, further studies involving simultaneous recordings of population oscillations in striatum, GP and STN are critical to test the hypothesis that the STN and output nuclei are engaged through the cortico-striato-pallidal route or cortico-subthalamic pathway according to the state of cortical or forebrain activation and the frequency of interaction. Nonetheless, the apparent dynamic nature of functional connectivity within cortico-basal ganglia circuits, in which both the components of a given circuit and the net direction of interaction may change, serves to illustrate the need for models of basal ganglia function that are not solely based on fixed and/or unidirectional influences.

References

- Alexander GE & Crutcher MD (1990). Functional architecture of basal ganglia circuits: neural substrates of parallel processing. *Trends Neurosci* **13**, 266–271.
- Bar-Gad I, Morris G & Bergman H (2003). Information processing, dimensionality reduction and reinforcement learning in the basal ganglia. *Prog Neurobiol* **71**, 439–473.
- Bergman H, Feingold A, Nini A, Raz A, Slovlin H, Abeles M, Vaadia E *et al.* (1998). Physiological aspects of information processing in the basal ganglia of normal and parkinsonian primates. *Trends Neurosci* **21**, 32–38.
- Berke JD, Okatan M, Skurski J & Eichenbaum HB (2004). Oscillatory entrainment of striatal neurons in freely moving rats. *Neuron* **43**, 883–896.
- Bevan MD, Booth PAC, Eaton SA & Bolam JP (1998). Selective innervation of neostriatal interneurons by a subclass of neuron in the globus pallidus of the rat. *J Neurosci* **19**, 9438–9452.
- Bevan MD, Magill PJ, Terman D, Bolam JP & Wilson CJ (2002). Move to the rhythm: oscillations in the subthalamic nucleus-external globus pallidus network. *Trends Neurosci* **25**, 525–531.
- Bolam JP, Hanley JJ, Booth PA & Bevan MD (2000). Synaptic organisation of the basal ganglia. *J Anat* **196**, 527–542.
- Boraud T, Bezard E, Bioulac B & Gross CE (2002). From single extracellular unit recording in experimental and human Parkinsonism to the development of a functional concept of the role played by the basal ganglia in motor control. *Prog Neurobiol* **66**, 265–283.
- Brown P (2003). Oscillatory nature of human basal ganglia activity: relationship to the pathophysiology of Parkinson's disease. *Mov Disord* **18**, 357–363.
- Brown P, Kupsch A, Magill PJ, Sharott A, Harnack D & Meissner W (2002). Oscillatory local field potentials recorded from the subthalamic nucleus of the alert rat. *Exp Neurol* **177**, 581–585.

- Brown P, Oliviero A, Mazzone P, Insola A, Tonali P & Di Lazzaro V (2001). Dopamine dependency of oscillations between subthalamic nucleus and pallidum in Parkinson's disease. *J Neurosci* **21**, 1033–1038.
- Buzsáki G & Draguhn A (2004). Neuronal oscillations in cortical networks. *Science* **304**, 1926–1929.
- Cassidy MJ & Brown P (2002). Hidden Markov based autoregressive analysis of stationary and non-stationary electrophysiological signals for functional coupling studies. *J Neurosci Meth* **116**, 35–53.
- Cassidy MJ & Brown P (2003). Spectral phase estimates in the setting of multidirectional coupling. *J Neurosci Meth* **127**, 95–103.
- Cassidy M, Mazzone P, Oliviero A, Insola A, Tonali P, Di Lazzaro V *et al.* (2002). Movement-related changes in synchronization in the human basal ganglia. *Brain* **125**, 1235–1246.
- Chudler EH, Sugiyama K & Dong WK (1993). Nociceptive responses in the neostriatum and globus pallidus of the anesthetized rat. *J Neurophysiol* **69**, 1890–1903.
- Courtemanche R, Fujii N & Graybiel AM (2003). Synchronous, focally modulated beta-band oscillations characterize local field potential activity in the striatum of awake behaving monkeys. *J Neurosci* **23**, 11741–11752.
- Donoghue JP & Wise SP (1982). The motor cortex of the rat: cytoarchitecture and microstimulation mapping. *J Comp Neurol* **212**, 76–88.
- Engel AK, Fries P & Singer W (2001). Dynamic predictions: oscillations and synchrony in top-down processing. *Nat Rev Neurosci* **2**, 704–716.
- Fujimoto K & Kita H (1993). Response characteristics of subthalamic neurons to the stimulation of the sensorimotor cortex in the rat. *Brain Res* **609**, 185–192.
- Goldberg JA, Rokni U, Boraud T, Vaadia E & Bergman H (2004). Spike synchronization in the cortex-basal ganglia networks of parkinsonian primates reflects global dynamics of the local field potentials. *J Neurosci* **24**, 6003–6010.
- Goto Y & O'Donnell P (2001). Network synchrony in the nucleus accumbens in vivo. *J Neurosci* **21**, 4498–4504.
- Graybiel AM (1995). Building action repertoires: memory and learning functions of the basal ganglia. *Curr Opin Neurobiol* **5**, 733–741.
- Haber SN (2003). The primate basal ganglia: parallel and integrative networks. *J Chem Neuroanat* **26**, 317–330.
- Halliday DM, Rosenberg JR, Amjad AM, Breeze P, Conway BA & Farmer SF (1995). A framework for the analysis of mixed time series/point process data – theory and application to the study of physiological tremor, single motor unit discharges and electromyograms. *Prog Biophys Mol Biol* **64**, 237–278.
- Horikawa K & Armstrong WE (1991). A biocytin-containing compound N-(2-aminoethyl) biotinimide for intracellular labeling and neuronal tracing studies: comparison with biocytin. *J Neurosci Meth* **37**, 141–150.
- Hubbard JI, Llinás R & Quastel DMJ (1969). Extracellular field potentials in the central nervous system. *Electrophysiological Analysis of Synaptic Transmission*, pp. 265–293. Edward Arnold Ltd, London.
- Kaminski MJ & Blinowska KJ (1991). A new method of the description of the information flow in the brain structures. *Biol Cybern* **65**, 203–210.
- Kasanetz F, Riquelme LA & Murer MG (2002). Disruption of the two-state membrane potential of striatal neurones during cortical desynchronization in anaesthetized rats. *J Physiol* **543**, 577–589.
- Kelly RM & Strick PL (2004). Macro-architecture of basal ganglia loops with the cerebral cortex: use of rabies virus to reveal multisynaptic circuits. *Prog Brain Res* **143**, 449–459.
- Kita H & Kita T (2001). Number, origins, and chemical types of rat pallidostriatal projection neurons. *J Comp Neurol* **437**, 438–448.
- Kita H & Kitai ST (1994). The morphology of globus pallidus projection neurons in the rat: an intracellular staining study. *Brain Res* **636**, 308–319.
- Kolomiets BP, Deniau JM, Glowinski J & Thierry AM (2003). Basal ganglia and processing of cortical information: functional interactions between trans-striatal and trans-subthalamic circuits in the substantia nigra pars reticulata. *Neuroscience* **117**, 931–938.
- Kühn AA, Williams D, Kupsch A, Limousin P, Hariz M, Schneider GH, Yarrow K & Brown P (2004). Event-related beta desynchronization in human subthalamic nucleus correlates with motor performance. *Brain* **127**, 735–746.
- Levy R, Ashby P, Hutchison WD, Lang AE, Lozano AM & Dostrovsky JO (2002). Dependence of subthalamic nucleus oscillations on movement and dopamine in Parkinson's disease. *Brain* **125**, 1196–1209.
- Magill PJ, Bolam JP & Bevan MD (2000). Relationship of activity in the subthalamic nucleus-globus pallidus network to cortical electroencephalogram. *J Neurosci* **20**, 820–833.
- Magill PJ, Bolam JP & Bevan MD (2001). Dopamine regulates the impact of the cerebral cortex on the subthalamic nucleus-globus pallidus network. *Neuroscience* **106**, 313–330.
- Magill PJ, Sharott A, Bevan MD, Brown P & Bolam JP (2004a). Synchronous unit activity and local field potentials evoked in the subthalamic nucleus by cortical stimulation. *J Neurophysiol* **92**, 700–714.
- Magill PJ, Sharott A, Bolam JP & Brown P (2004b). Brain state-dependency of coherent oscillatory activity in the cerebral cortex and basal ganglia of the rat. *J Neurophysiol* **92**, 2122–2136.
- Mahon S, Deniau JM & Charpier S (2001). Relationship between EEG potentials and intracellular activity of striatal and cortico-striatal neurons: an in vivo study under different anesthetics. *Cereb Cortex* **11**, 360–373.
- Marsden JF, Limousin-Dowsey P, Ashby P, Pollak P & Brown P (2001). Subthalamic nucleus, sensorimotor cortex and muscle interrelationships in Parkinson's disease. *Brain* **124**, 378–388.
- Mena-Segovia J, Bolam JP & Magill PJ (2004). Pedunculopontine nucleus and basal ganglia: distant relatives or part of the same family? *Trends Neurosci* **27**, 585–588.
- Mima T, Matsuoka T & Hallett M (2001). Information flow from the sensorimotor cortex to muscle in humans. *Clin Neurophysiol* **112**, 122–126.
- Mitzdorf U (1985). Current-source density method and application in cat cerebral cortex: investigation of evoked potentials and EEG phenomena. *Physiol Rev* **65**, 37–100.
- Murer MG, Tseng KY, Kasanetz F, Belluscio M & Riquelme LA (2002). Brain oscillations, medium spiny neurons, and dopamine. *Cell Mol Neurobiol* **22**, 11–32.

- Nambu A, Tokuno H, Hamada I, Kita H, Imanishi M, Akazawa T, Ikeuchi Y & Hasegawa N (2000). Excitatory cortical inputs to pallidal neurons via the subthalamic nucleus in the monkey. *J Neurophysiol* **84**, 289–300.
- Nambu A, Tokuno H & Takada M (2002). Functional significance of the cortico-subthalamo-pallidal 'hyperdirect' pathway. *Neurosci Res* **43**, 111–117.
- Paxinos G & Watson C (1986). *The Rat Brain in Stereotaxic Coordinates*, 2nd edn. Academic Press, Sydney.
- Sato F, Lavalley P, Levesque M & Parent A (2000). Single-axon tracing study of neurons of the external segment of the globus pallidus in primate. *J Comp Neurol* **417**, 17–31.
- Shink E, Bevan MD, Bolam JP & Smith Y (1996). The subthalamic nucleus and the external pallidum: two tightly interconnected structures that control the output of the basal ganglia in the monkey. *Neuroscience* **73**, 335–357.
- Smith Y, Bevan MD, Shink E & Bolam JP (1998). Microcircuitry of the direct and indirect pathways of the basal ganglia. *Neuroscience* **86**, 353–387.
- Smith Y, Raju DV, Pare JF & Sidibe M (2004). The thalamostriatal system: a highly specific network of the basal ganglia circuitry. *Trends Neurosci* **27**, 520–527.
- Steriade M (2000). Corticothalamic resonance, states of vigilance and mentation. *Neuroscience* **101**, 243–276.
- Stern EA, Jaeger D & Wilson CJ (1998). Membrane potential synchrony of simultaneously recorded striatal spiny neurons in vivo. *Nature* **394**, 475–478.
- Stern EA, Kincaid AE & Wilson CJ (1997). Spontaneous subthreshold membrane potential fluctuations and action potential variability of rat corticostriatal and striatal neurons in vivo. *J Neurophysiol* **77**, 1697–1715.
- Tseng KY, Kasanetz F, Kargieman L, Riquelme LA & Murer MG (2001). Cortical slow oscillatory activity is reflected in the membrane potential and spike trains of striatal neurons in rats with chronic nigrostriatal lesions. *J Neurosci* **21**, 6430–6439.
- Urbain N, Gervasoni D, Soulière F, Lobo L, Rentéro N, Windels F *et al.* (2000). Unrelated course of subthalamic nucleus and globus pallidus neuronal activities across vigilance states in the rat. *Eur J Neurosci* **12**, 3361–3374.
- West MO (1998). Anesthetics eliminate somatosensory-evoked discharges of neurons in the somatotopically organized sensorimotor striatum of the rat. *J Neurosci* **18**, 9055–9068.
- Williams D, Kühn A, Kupsch A, Tijssen M, van Bruggen G, Speelman H, Hotton G, Yarrow K & Brown P (2003). Behavioural cues are associated with modulations of synchronous oscillations in the human subthalamic nucleus. *Brain* **126**, 1975–1985.

Acknowledgements

This work was supported by the Medical Research Council UK (P.J., J.P.B. and P.B.) and the Brain Research Trust (A.S). P.J. holds a *Fellowship by Examination* at Magdalen College, Oxford. We thank L. Norman, C. Francis and B. Micklem for technical assistance.